

# Frequency-Locked Loop Between a H-Maser and a Cs Clock

J. Saalaoui<sup>1</sup>, M. Addouche<sup>1</sup>, F. Lardet-Vieudrin<sup>2</sup>  
 E. Rubiola<sup>3</sup>, V. Giordano<sup>2</sup> and F. Vernotte<sup>1</sup>

<sup>1</sup>Laboratoire d'Astrophysique de l'Observatoire de Besançon, LAOB, UMR-6091  
 41bis, av. de l'Observatoire, BP1615, F-25010 Besançon, France

e-mail : saalaoui@obs-besancon.fr

<sup>2</sup>dept. LPMO, Institut FEMTO-ST, UMR-6174, 32 av. de l'Observatoire, F-25044 Besançon, France.

<sup>3</sup>Université Henri Poincaré, ESSTIN and LPMIA

2 av. Jean Lamour, F-54519 Vandoeuvre Lès Nancy, France

**Abstract**— The time and frequency reference in Besançon is based on Cesium clocks for absolute accuracy and long-term stability, on a H-maser for medium and long term stability, and on a liquid-He whispering gallery sapphire oscillator for best spectral purity and short-term stability. These standards are located in three different places. In order to obtain the full accuracy and stability at least in one site, we combine these references using a frequency locked loop.

The traditional method consists of locking a VCO to a reference. The short-term stability of the VCO and the long term performance of the reference are therefore combined in the output signal, when the cut-off frequency of the control is properly chosen. Yet, in our case we have to lock the VCO to two references, the H-maser in the medium term and the Cs clock in the long term.

The control system consists of two mixers that compare the references to a quartz oscillator (VCO), and of a recursive digital filter. The H-maser and the Cs clock are not controlled.

This paper analyzes the method for choosing a suitable control algorithm, and presents the results based on simulated data.

## I. INTRODUCTION

LPMO, LCEP and LAOB are cooperating in time and frequency research in Besançon. Each laboratory has its own frequency standards. In the LAOB, there are three HP-5071A-001 Cs clocks, which provide the highest accuracy and long-term stability ( $\tau > 1$  day). These clocks contribute to TAI through differential GPS. The EFOS-21 H-maser at the LCEP shows high medium-term stability (parts in  $10^{-15}$  for  $\tau$  in the  $10^2$ - $10^5$  range). The cryogenic sapphire oscillators at the LPMO exhibits the lowest phase noise and the best short-term accuracy  $7 \times 10^{-15}$ . Yet this oscillator cannot be operated continuously.

Figure 1 shows the Allan deviation  $\sigma_y(\tau)$  of the available standards, as a function of the measurement time  $\tau$ . Fig. 2 shows the two-way frequency distribution network in Besançon.

Several works have been already achieved in order to build an atomic time-scale which combine the best performances of the cesium clock and that of maser clock [1], [2]. To build a such time-scale, we propose to lock a VCO on both these references.

From the comparison of the Cs and the H-maser, we can only know the difference  $y_{cs}(t) - y_{hm}(t)$ . Assuming that the

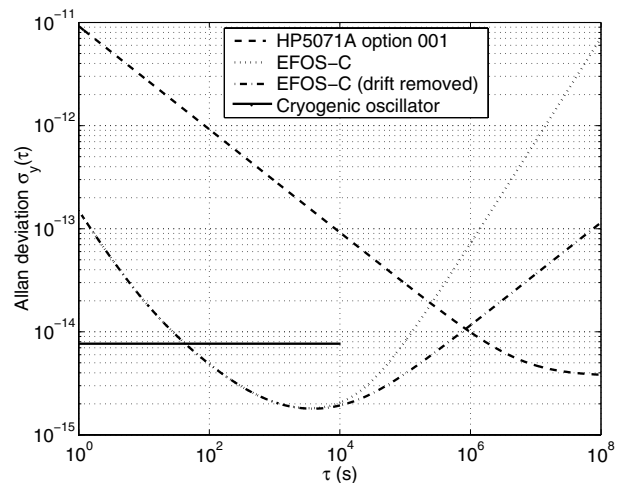


Fig. 1. Measured Allan deviation  $\sigma_y(t)$  of the available frequency references.

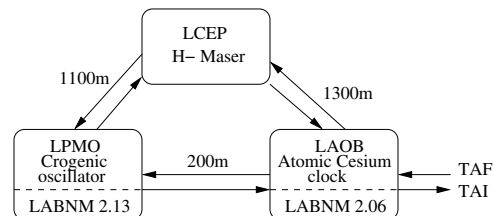


Fig. 2. Optical link between the three laboratories. Distances refer to fiber length, through underground path.

long term instabilities are only due to the H-maser, we can assess the quantity  $\hat{y}_{hm}(t)$  by applying a low pass filter to  $y_{cs}(t) - y_{hm}(t)$ . The cut-off frequency  $f_c$  is chosen in such a way that  $S_{yhm}(f) > S_{y_{cs}}(f)$  (see figure 3) for Fourier frequency lower than  $f_c$  (see figure 4). Unfortunately the H-maser may not be corrected by the estimate  $\hat{y}_{hm}(t)$  because it must remain in a free running mode. Then, we need a quartz oscillator (VCO) in order to take into account this correction. The VCO is simultaneously compared to the Cs and the H-maser and is

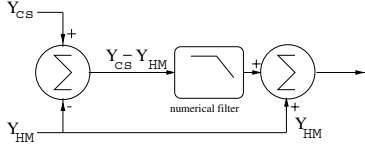


Fig. 3. Comparison of the Cs and H-maser.

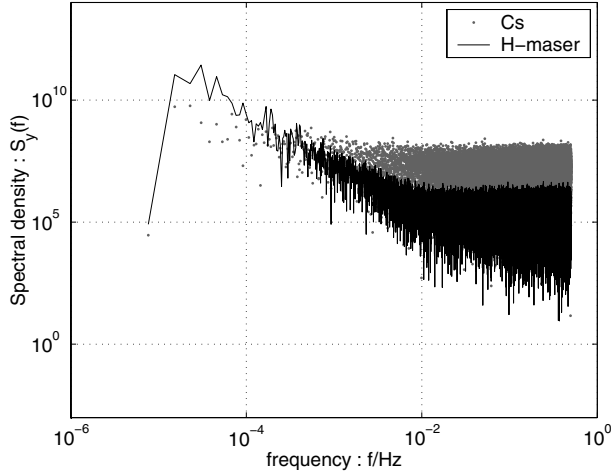


Fig. 4. Power density frequency of the Cs and H-maser.

corrected according to (figure 5).

The comparison of the VCO and Cs provides  $y_{cs}(t) - y_q(t)$ . The comparison of the VCO and H-maser provides  $y_{hm}(t) - y_q(t)$ .

The subscripts *hm*, *cs* and *q* stand for H-maser, Cesium, and quartz oscillator, respectively.

The difference of these quantity yields

$$[y_{cs}(t) - y_q(t)] - [y_{hm}(t) - y_q(t)] = y_{cs}(t) - y_{hm}(t)$$

After low pass filtering we obtain the estimate  $\hat{y}_{hm}(t)$  which is subtracted from  $y_{hm}(t) - y_q(t)$ .

We get then on estimate of  $-y_q(t)$  which can be used for correcting the VCO.

In this paper, we propose a method for adjusting then cut-off frequency  $f_c$ .

This method will be studied from numerical simulations.

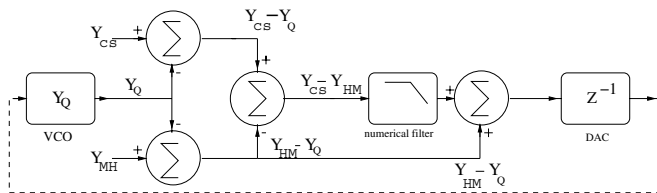


Fig. 5. Three steps of control.

## II. METHOD

### A. Control oscillator equation

The angular frequency of VCO is expressed at a given  $t$  in the following equation:

$$\omega_q(t) = \omega_0(t) + k_f \int_0^t v(u) du, \quad (1)$$

where  $\omega_0$  is the free pulsation of the oscillator, and  $k_f$  is the sensitivity of the VCO. The voltage command at the exit of the corrector will be:

$$v(t) = k_d \{ [y_{cs}(t) - y_{hm}(t)] * g(t) + [y_{hm}(t) - y_q(t)] \}, \quad (2)$$

where  $g(t)$  is the impulse response of the filter and  $k_d$  is expressed in V.

For the recursive numerical filter, the output signal of the filter will be:

$$y(t_n) = \frac{p_c}{1+p_c} [y_{cs}(t_n) - y_{hm}(t_n)] + \frac{p_c}{1+p_c} [y_{cs}(t_{n-1}) - y_{hm}(t_{n-1})] + \frac{1-p_c}{1+p_c} y(t_{n-1}), \quad (3)$$

where  $p_c$  is the low cut-off pulsation.

In order to calculate the value of the filtered signal at  $t_n$ , one needs this value at  $t_{n-1}$ , and also the values at  $t_n$  and  $t_{n-1}$  before filtering.

The filter cut-off frequency must be chosen in the interval of  $f_{min} = \frac{1}{N\tau_0}$  and  $f_{max} = \frac{1}{2\tau_0}$ , where  $N$  defines the samples count and  $\tau_0$  the sampling step.

The development of control oscillator equations consists of two analysis: a spectral analysis by a Laplace transform, and a temporal analysis by a z transform.

1) *The Laplace transform:* Transforming (1) gives:

$$\Omega_q(p) = \Omega_0(p) + \frac{k_f}{p} V(p). \quad (4)$$

By substitution with the Laplace transform of equation (2):

$$\Omega_q(p) = \Omega_0(p) + \frac{k_f}{p} [(\Omega_{cs}(p) - \Omega_{hm}(p)) G(p) + \Omega_{hm}(p) - \Omega_q(p)], \quad (5)$$

where  $G(p)$  is the transfer function of the filter.

By judicious arrangements, we get:

$$\Omega_q(p) = \frac{\tau p}{1 + \tau p} \Omega_0(p) + \frac{G(p)}{1 + \tau p} \Omega_{cs}(p) + \frac{1 - G(p)}{1 + \tau p} \Omega_{hm}(p), \quad (6)$$

where  $\tau = \frac{1}{k_f k_d}$ .

This equation shows two limit cases:

- In the long term ( $p \rightarrow 0$ ), the equation (6) yields:

$$\Omega_q(p) \rightarrow G(0) \Omega_{cs} + [1 - G(0)] \Omega_{hm} \simeq \Omega_{cs}, \quad (7)$$

because  $G(p) = G(0) = \frac{p_c}{p + p_c} \rightarrow 1$ .

- In the short-term ( $p \rightarrow \infty$ ) equation (6) yields:

$$\Omega_q(p) \rightarrow \Omega_0 + \frac{G(p)}{\tau p} \times \Omega_{cs} + \frac{1 - G(p)}{\tau p} \Omega_{hm} \simeq \Omega_q. \quad (8)$$

2)  $z$  transform: The Laplace domain equation (5) gives:

$$\omega_q(z) = \omega_0(z) + \frac{k_f}{p} [(\omega_{cs}(z) - \omega_{hm}(z)) G(p) + (\omega_{hm}(z) - \omega_q(z))] . \quad (9)$$

Substituting  $p$  by  $\frac{z-1}{z+1}$ , we obtain:

$$\omega_q(z) = \omega_0(z) + k_f \frac{z+1}{z-1} [(\omega_{cs}(z) - \omega_{hm}(z)) G(p) + \omega_{hm}(z) - \omega_c(z)] .$$

Substituting  $z^{-1}w(z)$  by  $w(t_{n-1})$ , we obtain:

$$\begin{aligned} \omega_q(t_n) = & \frac{1+p_c}{1+k_f+p_c k_f} \omega_0(t_n) - \frac{2}{1+K_f+p_c k_f} \omega_q(t_n-1) + \\ & + \frac{1-p_c}{1+k_f+p_c k_f} \omega_0(t_n-2) + \frac{k_f}{1+k_f+p_c k_f} \omega_{hm}(t_n) + \\ & - \frac{k_f}{1+k_f+p_c k_f} \omega_{hm}(t_n-2) + \frac{k_f p_c}{1+k_f+p_c k_f} [\omega_{cs}(t_n)] + \\ & + 2\omega_{cs}(t_{n-1}) + \omega_{cs}(t_{n-2}) + \frac{2(1-p_c k_f)}{1+k_f+p_c k_f} \omega_q(t_{n-1}) + \\ & + \frac{p_c+k_f-k_f p_c-1}{1+k_f+p_c k_f} \omega_{cs}(t_n) . \end{aligned} \quad (10)$$

When the Fourier frequency is higher than the cut-off frequency  $f_c$ , the quartz is locked on the H-Maser. If it is lower than  $f_c$ , the quartz is locked on the Cs.

### III. SIMULATION

#### A. Noise generation of the 3 clocks

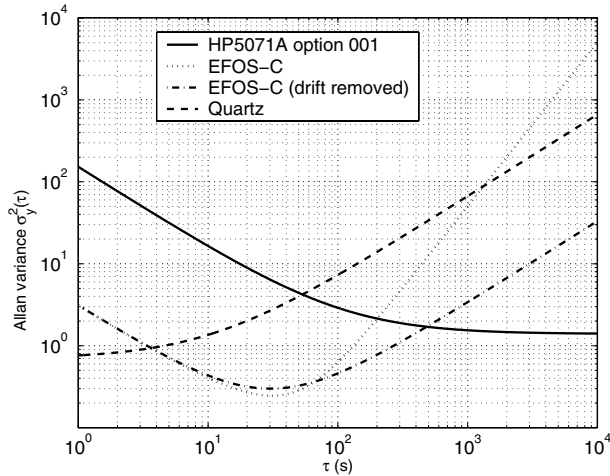


Fig. 6. Theoretical Allan variance of the 3 clocks simulated and normalized.

The frequency fluctuation of our standards are described by the power-law model

$$S_{y_i}(f) = \sum_{\alpha=-2}^{+2} h_{\alpha i} f^{\alpha} \quad \text{for } i = 1 \text{ to } 3 , \quad (11)$$

noise type	Cs clock	H-maser clock	Quartz
white $h_0$	300	6	0
flicker $h_{-1}/f$	1	$7.210^{-2}$	0.5
random walk $h_{-2}/f^2$	0	$5.10^{-4}$	$10^{-2}$

TABLE I

LEVELS NOISE OF THE THREE CLOCKS

where  $i$  indicates the clock.

Due to technical difficulties, the estimation has been performed on only 3000 samples, it is for what, the results and also the curves are normalised into a changed noise levels values (figure 1 vs figure 6).

We generate three sets of samples ( $y_q(t)$ ,  $y_{hm}(t)$  and  $y_{cs}(t)$ ) according to the noise level that correspond to the three clocks [3] we use (vco, H-maser and Cs).

We then used the frequency difference ( $y_{cs} - y_q$ ) and ( $y_{hm} - y_q$ ), to obtain ( $y_{cs} - y_{hm}$ ) by substraction. Table I shows the noise coefficients  $h_{\alpha i}$ .

The three obtained signals correspond to the sequences of instantaneous frequency deviations of the samples. The first one corresponds to the short-term stability, the second to medium-term stability, and finally the last represents the long-term stability (see figure 6).

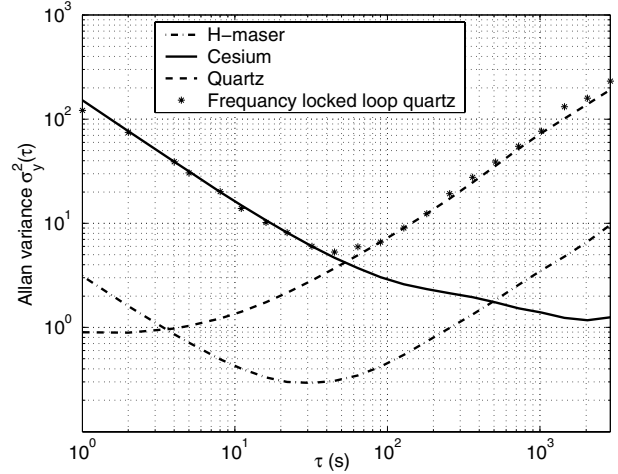


Fig. 7. Stability results unsatisfactory from a simulated ensemble of three clocks.

#### B. Discussion

The output signal (locked frequency) we obtain using our setup (figure 5) is formulated by equation (6). We notice that the shape of the output signal stability is function of the cut-off frequency  $f_c$  of the numerical filter and also of the oscillator sensitive coefficient  $k_f$ . We have seen before that, for lower frequency, the cut-off frequency  $f_c$  enables to select on which source the VCO is locked.

Equation (4) shows that the locked frequency  $\Omega_q(p)$  is composed of an integration of the correction signal  $V(p)$ . It is thus

subjected to a low filtering. The rate of this low filtering is fixed by the value of  $k_f$ .

Three clocks were simulated directly from equation (11) and table (I) (see figure 6). We have varying the values of  $k_f$  and  $f_c$  and then calculating the  $\Omega_q(t)$  (equation 6), as well as the Allan variance of the corrected oscillator. Figure 7 represents the worst results we obtain when varying the values of the couple  $(k_f, f_c)$ .

The best results (figure 8) are obtained when  $f_c$  has been fixed to the intersection value between the Power spectral density shape of the Cesium clock signal and that of the H-Maser ( $f_c = 2 \cdot 10^{-3}$ ). The value of  $k_f$  experimentally found to be  $3.4 \cdot 10^{-1}$  Hz.

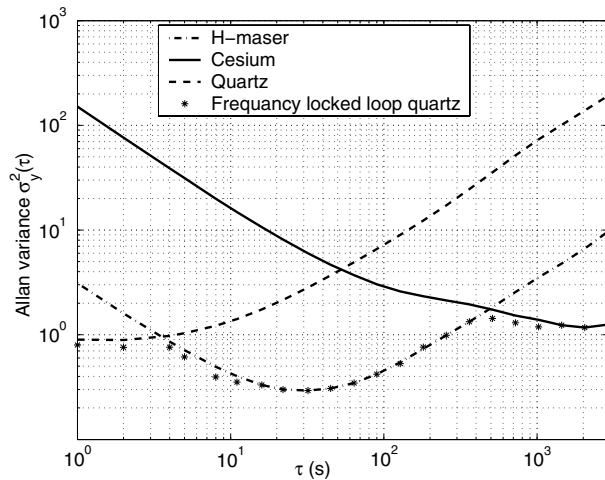


Fig. 8. Stability results from a simulated ensemble of three clocks.

#### IV. PHYSICAL REALIZATION

The device shown in the figure 9 represents the physical realization of the control system which is composed of the following components: two mixers, two narrow band filters, two Zero-Crossing detector ZCD and two frequency counters. With such a type of ZCD a time jitter level of few  $10^{-7}$  at 100 MHz is expected [4] [5]. In principle this scheme is able to estimate a frequency stability of less than of  $10^{-15}$ .

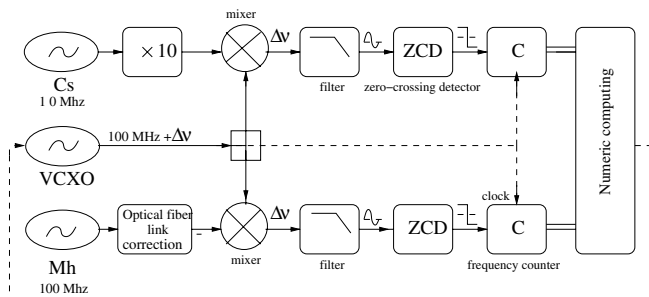


Fig. 9. Method of dual-mixer time difference (DMTD).

#### REFERENCES

- [1] Lee A. Breakiron, "Timescale algorithms combining cesium clocks and hydrogen masers", Proc. 23rd PTI pp. 297-305, NASA Conference Publication CP-3159, California, Dec. 1991.
- [2] M. A Weiss and F. Walls, "Preliminary evaluation of time scale based on hydrogen masers", Proc. 8 th EFTF pp. 297-305, Munich Germany, 1994.
- [3] F. Vernotte, E. Lantz, J. Gros Lambert and J.J. Gagnepain, "Oscillator noise analysis : multivariate measurement.", IEEE Transactions on Instrumentation and Measurement, IM-42 pp. 342-350, Avril. 1993.
- [4] S. Stein, D. Glaze, J. Levine, J. Gray, D. Howe and L. Erb, "Performance of an automated high accuracy phase measurement system", Proc. 36th FCS pp. 314-320, Philadelphia, Pennsylvania June. 1982.
- [5] G. Brida, "High resolution frequency stability measurement system", Review of Scientific Instruments Vol 73(5) pp. 2171-2174. May. 2002.